

Photocatalytic Oxidation of Acid Orange 10 dye Molecules using Cerium Oxide Nanosphere Particles under Ultraviolet and Visible Light Irradiations

M. Prathap Kumar, G.A. Suganya Josephine, A. Sivasamy*

Chemical Engineering Area, CSIR-Central Leather Research Institute, Adyar, Chennai 600020

*Correspondence author: E-mail: arumugamsivasamy@yahoo.co.in

DOI: 10.5185/amp.2019.0014

www.vbripress.com/amp

Abstract

Exploration of semiconductors in the field of photocatalysis plays a crucial role in energy and environmental remediation in particular oxidation/reduction of toxic organic contaminants from water and wastewater. The present research work aims on synthesis of pristine CeO₂ nanoparticles by precipitation method and was thoroughly characterized by Fourier Transform Infrared spectroscopy, X-ray Diffraction, UV-vis-Diffuse Reflectance Spectroscopy, High Resolution Scanning Electron Microscopy, EDAX and Electron Spin Resonance techniques. The band gap energy (E_{bg}) was found to be 3.19 eV. The synthesized nanomaterials showed spherical morphology and the particles size ranged from 50-93 nm. The insitu generation of ·OH radicals was confirmed from ESR studies. The synthesized CeO₂ nanospheres was evaluated in photocatalytic oxidation of an azo dye Acid orange 10 under Ultraviolet and visible light irradiations. Experimental studies such as pH, catalyst amount and effect of initial dye concentration were also studied. Kinetic studies indicate the photo reaction follows pseudo-first order rate equation. The photocatalytic oxidation of dye molecules were monitored by UV-visible spectroscopy and COD analyses. The level of chemical oxygen demand (COD) of the photodegraded samples decreases in both the photocatalytic systems indicating that dye molecules readily degraded under present experimental conditions. Effect of electrolytes like MgSO₄, KCl, Na₂CO₃ and NaHCO₃ were also investigated to check interference of inorganic anions on photocatalytic oxidation of dye molecules using CeO₂ nanospheres. Finally, the prepared catalyst was checked for its reusability and the photocatalyst exhibited better photocatalytic activity even after three cycles of regeneration. Copyright © VBRI Press.

Keywords: Semiconductors, photocatalysis, CeO₂ nanospheres, ultraviolet and visible light, dye degradation.

Introduction

The waste water released from industries such as textiles, tanneries and fine chemicals are contaminated with hazardous pollutants such as dyes, endocrine disruptors and heavy metals and are discharged into natural water causing major threat to environment [1]. The effluents were toxic in nature and cause various diseases to living beings [2]. Different methods have been adopted in treatment of wastewater but due to its disadvantages an alternative method has to be employed. Advanced Oxidation Process (AOP) through semiconductor photocatalysts is a promising and effective method in dye degradation [3]. Different heterogeneous photocatalysts like TiO₂, ZnO, CeO₂ [4] have been employed in Ultraviolet and visible light driven photocatalytic oxidation and reduction of contaminants present in waste water. Cerium oxide (CeO₂) rare earth metal oxide (band gap = 3.19 eV) exhibits high efficiency in visible and Ultraviolet light exhibits properties like multiple valence states [5-6] and oxygen storage capacity [7-9]. It also finds number of

applications such as solid oxide fuel cells, catalysis, oxygen sensors and also as photocatalyst in degradation of contaminants, hydrogen storage and thermal dissociation of H₂O and CO₂ [10-15]. In the present work a precipitation method was employed to synthesize pristine spherical CeO₂ nanoparticles and it was characterized by Fourier Transform Infrared spectroscopy, X-ray Diffraction, UV-vis-Diffuse Reflectance Spectroscopy, High Resolution Scanning Electron Microscopy, EDAX and Electron Spin Resonance techniques. The efficacy of CeO₂ was investigated in photocatalytic oxidation of acid orange 10 dye under Ultraviolet and Visible light irradiation.

Experimental section

Materials

Cerium nitrate hexahydrate (Ce(NO₃)₆·6H₂O 98%) and DMPO were procured from Sigma-Aldrich, India. Acid Orange 10 dye (AO10) and Sodium carbonate

(Na_2CO_3) were purchased from S.D. Fine Chem., Mumbai, India. All the chemicals were employed without purification. The purification of DMPO was performed and purity was checked before analysis.

Synthesis

Pristine CeO_2 was synthesized by precipitation method using cerium nitrate as a precursor and sodium carbonate as precipitating agent. A typical procedure is given below [16]: Equimolar solution of cerium nitrate and sodium carbonate was prepared. On addition of base to the cerium nitrate solution a white precipitate was obtained. The material was filtered and washed with water and ethanol. The CeO_2 was dried in hot air oven at 110°C overnight and calcined at 700°C for 3h and was named as PCeO_2 . The prepared PCeO_2 was stored in desiccator.

Characterization of the catalyst

The presence of surface functional groups in the synthesized PCeO_2 was measured by Fourier Transform Infrared spectroscopy (Perkin Elmer). The crystallinity and phase analysis were characterized by X-ray Diffraction (PAN analytical X-ray diffractometer, Germany). The band gap energy of PCeO_2 was analyzed by UV-visible-Diffuse Reflectance Spectroscopy (UV2600, Shimadzu spectrometer; Japan). The morphology, particle size and elemental composition were determined by High Resolution Scanning Electron Microscopy and EDAX analysis (Model Supra 55- Carl Zeiss, Germany). The generation of OH free radicals under UV and Visible irradiation was confirmed by Electron Spin Resonance techniques (Model - Bruker EMX X Band).

Photocatalytic oxidation of AO10 by PCeO_2

AO10 was oxidized photocatalytically under Ultraviolet and visible light irradiations. The reactions was conducted separately in annular batch type Ultraviolet and visible photoreactors. The source of visible light irradiation was a water cooled, 500 W tungsten filament lamp while 8 UV lamps (8 W each) at 254 nm were the source of UV irradiation. Cooling fans were provided in the reactor. Studies on effect of pH, catalyst loading and dye concentration were optimized based on preliminary photocatalytic experiments. Order of the reaction was determined from kinetic studies. Samples were withdrawn from the reaction solution and analysed by UV-visible spectroscopy. Using a calibration graph, the concentration of unreacted dye molecules in the solution was calculated and the percentage dye degradation was determined by the following equation:

$$\text{Degradation efficiency (\%)} = (C_0 - C_e / C_0) * 100 \quad (1)$$

where, C_0 and C_e are the initial and final dye concentrations in the aqueous phase, respectively.

Results and discussion

Fourier transform infrared spectroscopy

The Fourier Transform Infrared spectra of as synthesized PCeO_2 were recorded by disc plate method in the range of $400\text{-}4000\text{ cm}^{-1}$ employing KBr as an internal standard. The FT-IR spectra of PCeO_2 exhibits characteristic peaks at 848 and 521 cm^{-1} shown in **Fig. 1a**, which corresponds to metal oxide stretching vibrations of Ce-O in the synthesized catalyst. A band at 3453 cm^{-1} is attributed to the OH groups at the surface while peak at 1382 cm^{-1} corresponds to physically adsorbed water molecules [17].

X-ray diffraction

The XRD patterns of PCeO_2 exhibits peaks at 2θ scale at 28.43° , 33.14° , 47.63° , 56.31° , 59.04° and 69.53° corresponding to (111), (200), (220), (311), (222) and (400) planes respectively and is shown in **Fig. 1b**. The crystallite size was calculated using Scherrer eq. (2).

$$D = k\lambda / (B \cos \theta) \quad (2)$$

where, k is 0.94 (spherical nanoparticles), λ the wavelength of radiation (0.154 nm) and B is the full width at half maximum (FWHM) and θ half the diffraction angle. The average crystallite size of the as synthesized PCeO_2 was found to be 52-56 nm.

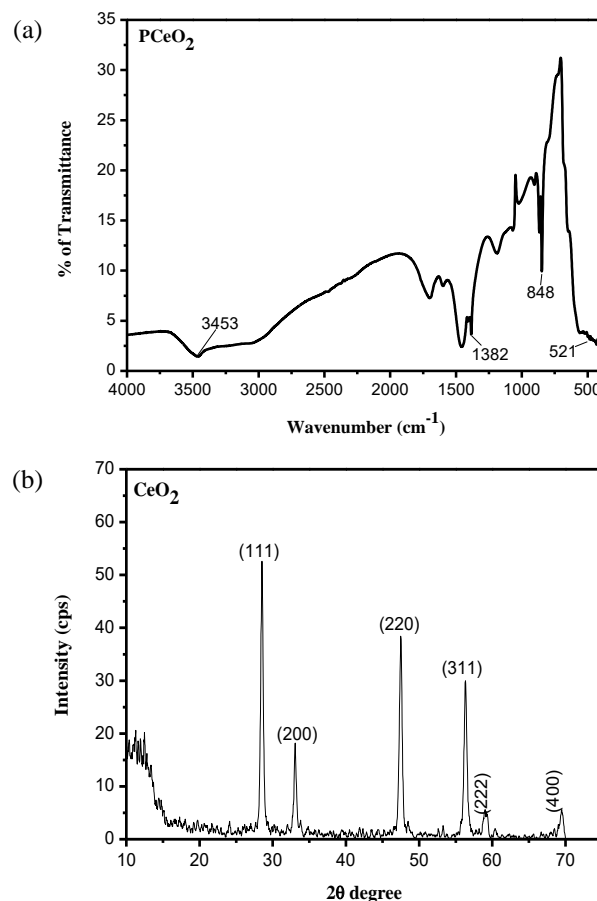


Fig. 1. (a) Fourier Transform Infrared spectrum and (b) X-Ray Diffraction pattern of PCeO_2 .

UV-visible diffuse reflectance spectroscopy (UV-vis-DRS)

The photocatalytic activity of the catalyst was investigated by absorption of light energy. The absorption characteristics are shown in the UV-visible diffuse reflectance spectrum of the prepared material (**Fig. 2a**) the amount of energy required for the excitation of the electron from valence band to conduction band is determined by band-gap energy (E_g). Crystalline CeO_2 shows an absorption maximum at around 400 nm in the UV region [18]. E_g was calculated from a plot of $(Ah\nu)^2$ vs $h\nu$ and is shown in **Fig. 2b**. The E_g of the synthesized PCeO_2 is 3.19 eV.

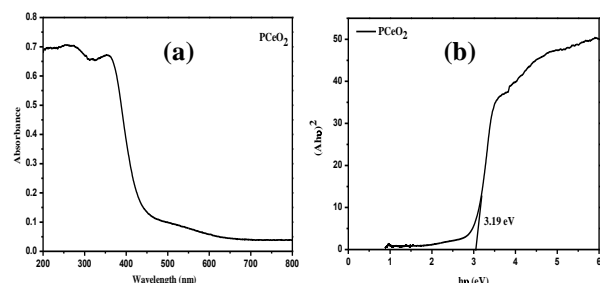


Fig. 2. (a) UV-vis- Diffuse Reflectance Spectrum and (b) Band gap of synthesized PCeO_2

Surface morphology by high resolution scanning electron microscopy and EDAX analysis

The HRSEM images indicates that PCeO_2 were spherical in shape and particle size of the synthesized was confirmed from analysis and is shown in **Fig. 3a**. The particle size ranges from 50-93 nm and displayed spherical morphology. The elemental composition confirms the presence of constituent elements in the synthesized material shown in **Fig. 3b**.

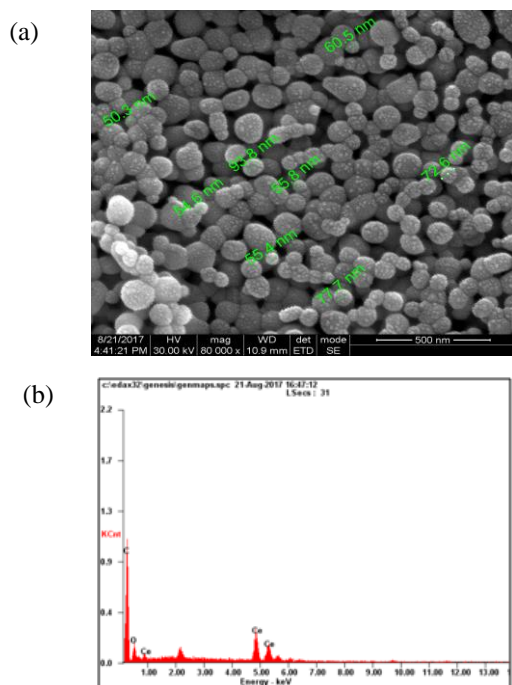


Fig. 3. Morphology of PCeO_2 (a) HRSEM and (b) EDAX analyses.

Electron spin resonance studies

The OH free radicals generated in the reaction medium on Ultraviolet or visible light irradiation were analyzed by Electron Spin Resonance analysis. The irradiation experiments were carried out in aqueous medium and DMPO was employed as a spin trapping agent. After addition of the photocatalyst, the mixture was irradiated with UV (60 s) or visible light (20 min). The samples were then centrifuged and the Electron Spin Resonance spectrum of the clear solutions were recorded. A characteristic four peak signal of intensity ratio of 1:2:2:1 was obtained as shown in **Fig. 4**. This represents the spin trapped DMPO- $\cdot\text{OH}$ radical adduct. This OH free radicals were formed in the system by photocatalyst upon light irradiation.

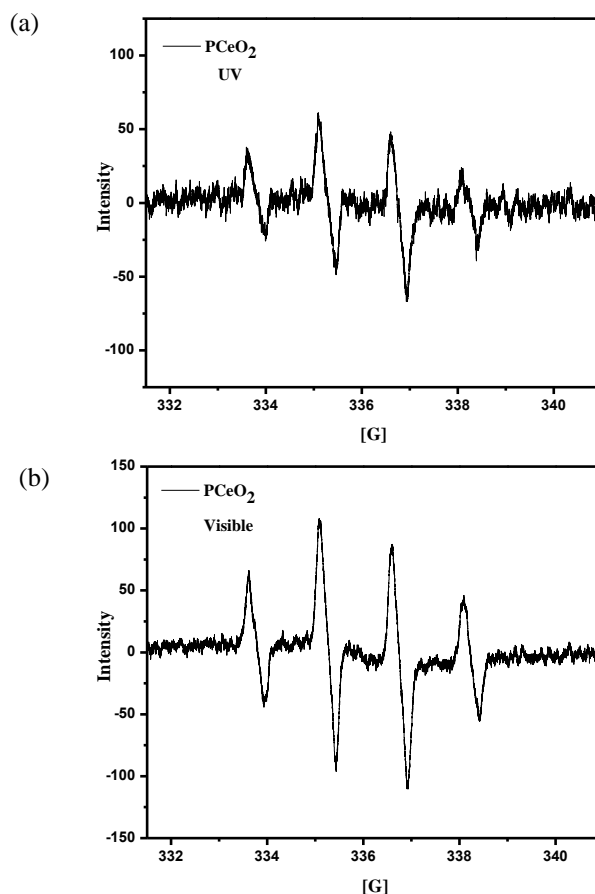


Fig. 4. Electron Spin Resonance spectrum of the DMPO spin trapped OH free radical formed under (a) Ultraviolet and (b) visible irradiation.

Photocatalytic activity

The characterization studies reveals that the synthesized PCeO_2 nanospheres exhibits a band gap value of 3.19 eV and particle size ranges from 50-93 nm. OH free radicals was formed in the photocatalytic system was confirmed from ESR spectroscopic studies. The OH free radicals further react with organic dyes resulting in mineralization process which leads to release of CO_2 and H_2O . Experimental studies such as variation of pH, varying catalyst loading and initial dye concentration

was determined out to investigate the optimum ratio suitable for photocatalytic oxidation of AO10 under Ultraviolet and Visible light irradiation.

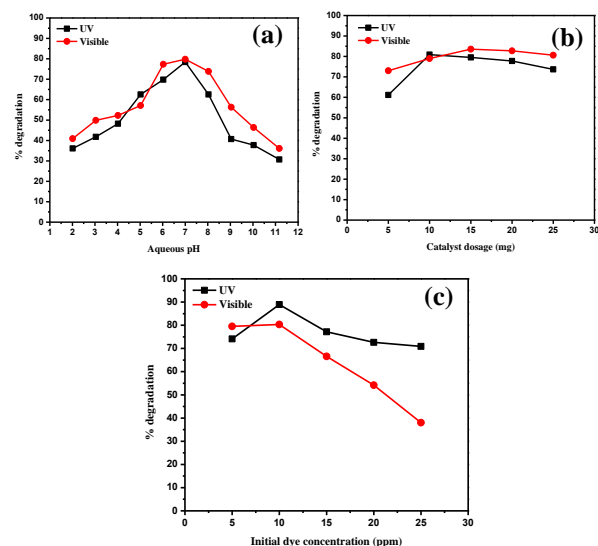


Fig. 5. Photocatalytic oxidation of AO10 dye by PCEO₂ under Ultraviolet and Visible light irradiation (a) Variation of pH, (b) Varying catalyst loading and (c) Effect of dye concentration.

Preliminary studies under Ultraviolet and Visible light irradiation

Studies on variation of pH

The photocatalytic oxidation of AO10 dye by PCEO₂ photocatalyst was subjected in a range of pH (2-11) under Ultraviolet and Visible light irradiations and is shown in **Fig. 5a**. The synthesized photocatalyst displayed 79% and 78% of degradation under Visible and Ultraviolet light irradiation at neutral pH. Hence neutral pH was fixed and further photocatalytic experiments were conducted at neutral pH.

Studies on varying catalyst loading

Studies on varying catalyst loading in photocatalytic oxidation of AO10 dye was displayed in **Fig. 5b**. The catalyst amount was varied from 5 - 25 mg/ 10 ml of 10ppm dye concentration. 83.55% and 80.86% of degradation was exhibited by 15 mg and 10 mg of PCEO₂ under Visible and Ultraviolet light irradiation. On further increasing the catalyst amount, decrease in percentage of degradation was observed and is due to large amount of substance that may obstruct the light entering the system, thereby reducing the photocatalytic degradation. Hence 10 mg and 15 mg of catalyst dosage was chosen as the optimum quantity for photocatalytic oxidation of AO10 under Ultraviolet and Visible light irradiations respectively.

Studies on varying dye concentration

Studies on varying initial dye concentration for 10 ml of test solution with optimum amount of catalyst under neutral pH was varied from 5-25 mg/L. Further on increasing the concentration of dye, decrease in percentage of degradation was observed from 88.94 -

70.88% and 80.32 - 38% was observed under Ultraviolet and Visible light irradiation respectively at neutral pH and is shown in **Fig. 5c**. Hence 10 mg and 15 mg/ 10 ml at neutral pH was fixed as optimum quantity in photocatalytic oxidation of AO10 under Ultraviolet and Visible light irradiation respectively.

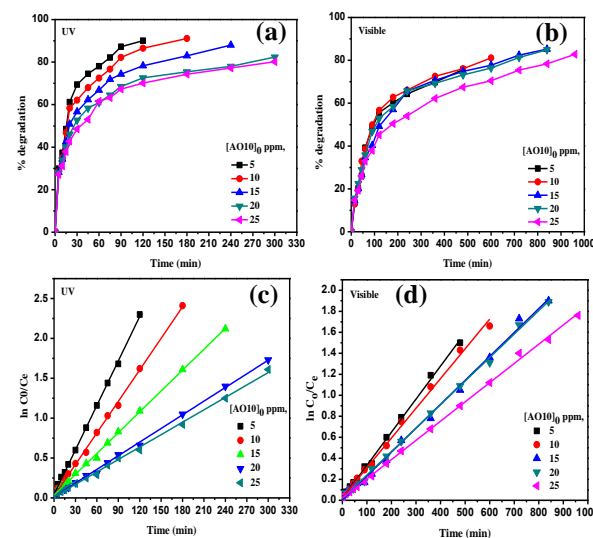


Fig. 6. Kinetics of photo oxidation of AO10 (a) Ultraviolet (b) Visible. Pseudo- first order kinetic plots for photo oxidation of AO10 under (c) Ultraviolet (d) Visible light irradiation.

Kinetics

The photocatalytic oxidation of AO10 by PCEO₂ was determined by time dependence studies. The kinetics were performed for various initial dye concentrations ranging from 5-25 ppm with 100 mg and 150 mg of PCEO₂ in 100 ml dye concentration at neutral pH in the photocatalytic system and the results were displayed in **Fig. 6a** and **Fig. 6b**. Kinetics obeyed pseudo-first order pathway **Fig. 6c** and **Fig. 6d**. The samples collected during kinetic studies were analyzed by UV-visible absorbance and COD analysis and the results were displayed in **Fig. 7a**, **Fig. 7b** and **Fig. 7c** respectively.

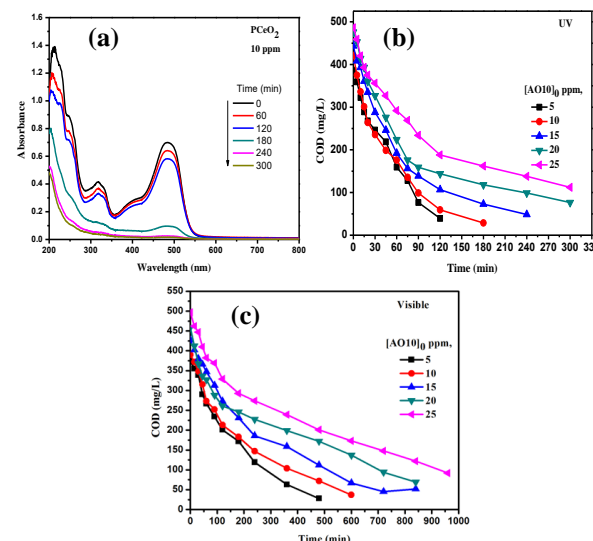


Fig. 7. (a) UV- Visible absorbance spectrum, Decrease in COD value under (b) Ultraviolet (c) Visible.

COD value decreases from 390 mg/L to 37 mg/L and 421.2 mg/L to 28.8 mg/L in Ultraviolet and Visible light for 10 ppm of dye concentration. The UV-visible spectrum suggests that the AO10 dye molecule was mineralized completely and absence of peaks in the scan range of 200-800 nm in the spectrum.

Effect of electrolytes on photocatalytic oxidation of AO10

The interference of inorganic anions on photocatalytic oxidation of AO10 by PCeO_2 was investigated in the presence of KCl , MgSO_4 , Na_2CO_3 and NaHCO_3 and is shown in Fig. 8. The concentrations of electrolytes were varied from 1-7 wt% with 10 mg and 15 mg of PCeO_2 under Ultraviolet and Visible light respectively in 10 ppm dye concentration. Increasing the concentration of KCl resulted in decrease in percentage of degradation [19], the percentage of degradation increased in case of carbonates by increase in its concentration. The concentration of sulphate increased upto 1.5% and decrease in photocatalytic degradation was observed and is due to presence of sulphate radicals which may be produced in the photocatalytic system at lower concentration.

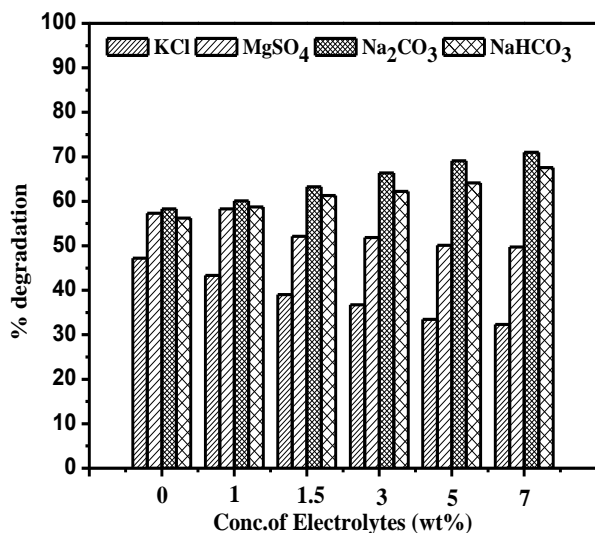


Fig. 8. Studies on electrolytes addition on photocatalytic oxidation of AO10 dye by PCeO_2 .

Reusability studies

The efficacy of PCeO_2 on photocatalytic oxidation of AO10 was determined from reusability studies and is shown in Fig. 9 (a) and 9 (b). The catalyst exhibits better activity even after three cycles. PCeO_2 showed decrease in percentage of degradation from 85% to 83% in Ultraviolet and 78% to 76% in Visible light irradiation. The results indicates that the catalyst was photocatalytically active even after three cycles of regeneration.

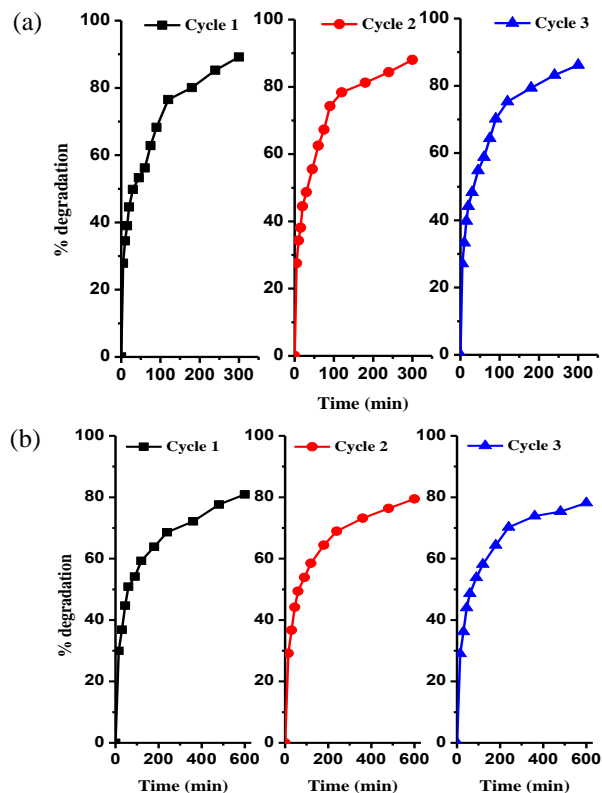


Fig. 9. Reusability studies of PCeO_2 in photocatalytic oxidation of AO10 under (a) Ultraviolet and (b) Visible light irradiation.

Summary

Precipitation method was employed in synthesis of PCeO_2 nanospheres and characterized by Fourier Transform Infrared spectroscopy, X-ray Diffraction, UV-vis-Diffuse Reflectance Spectroscopy, High Resolution Scanning Electron Microscopy, EDAX and Electron Spin Resonance techniques. The average crystallite size was 52-56 nm and band gap energy (E_g) was found to be 3.19 eV. The particle size was in nano range (50-93 nm) and displayed spherical morphology and EDAX analysis confirms the presence of constituent elements. The OH radicals generated was confirmed from Electron Spin Resonance studies. Further the synthesized PCeO_2 nanospheres was evaluated for its activity in photocatalytic oxidation of AO10 dye under Ultraviolet and Visible light irradiation. 10 mg and 15 mg of PCeO_2 exhibits 88.94% and 80.32% of degradation under Ultraviolet and visible light irradiation for 10 ppm dye concentration respectively. The reaction followed pseudo-first order relationship which is confirmed from kinetic studies. Decrease in COD from 390 mg/L to 37 mg/L and 421.2 mg/L to 28.8 mg/L under Ultraviolet and Visible light was obtained confirming the progress of reaction. The photocatalyst retained its photocatalytic activity which is confirmed from reusability studies. Hence the prepared PCeO_2 nanospheres exhibits better degradation in Ultraviolet light in degrading organic moiety present in waste water compared to Visible light.

References

1. Zaharia, D.; Suteu, A.; Muresan, R.; Muresan, A.; Popescu; Environ. Eng. Manage. J.; **2009**, *8*, 1359.
2. Stylidi, M.; Kondarides, D.I.; Verykios, X.E.; *Appl. Catal. B.*, **2004**, *47*, 189.
3. Philippe, C.; Vandevivere, B.; Willy, V.; *J. Chem. Technol. Biotechnol.*, **1998**, *72*, 289.
4. Lathasree, S.; Nageswara, R.; Sivasankar, B.; Sadasivam, V.; Rengaraj, K.; *J. Mol. Catal. A: Chem.*, **2004**, 223,101.
5. Laachir, A.; Perrichon, V.; Badri, A.; *J. Chem. Soc., Faraday Trans.*, **1991**, *87*, 1601.
6. Kubsh, J. E.; Rieck, J. S.; Spencer, N. D.; *Stud. Surf. Sci. Catal.*, **1991**, *71*, 125.
7. Kaspar, J.; Fornasiero, P.; Graziani, M.; *Catal. Today*, **1999**, *50*, 285.
8. Arias, M.; Garcia, F. M.; Hungria, A. B.; Juez, A. I.; Duncan, K.; Smith, R.; *J. Catal.*, **2001**, *204*, 238.
9. Li, G. F.; Wang, Q. Y.; Zhao, B.; Zhou, R. X.; *Fuel*, **2012**, *92*, 360.
10. Chueh, W. C.; Falter, C.; Abbott, M.; Scipio, D.; Furler, P.; Haile, S. M.; Steinfeld, A.; *Science*, **2010**, *330*, 1797.
11. Chueh, W. C.; Haile, S. M.; *Chem Sus Chem.*, **2009**, *2*, 735.
12. Scheffe, J. R.; Steinfeld, A.; *Energ & Fuel.*, **2012**, *26*, 1928.
13. Zhang, D.; Du, X.; Shi, L.; Gao, R.; *Dalton Trans.*, **2012**, *41*, 14455.
14. Muhich, C. L.; Evanko, B. W.; Weston, K. C.; Lichty, P.; Liang, X.; Martinek, J.; Musgrave, C. B.; Weimer, A. W.; *Science*, **2013**, *341*, 540.
15. Latha, P.; Prakash, K.; Karuthapandian, S.; *Adv. Powder Technol.*, **2017**, *28*, 2903.
16. Anandan, S.; Vinua, A.; Sheeja Lovely, K.L.P.; Gokulakrishnan, N.; Srinivasu, P.; Mori, T.; Murugesan, V.; Sivamurugan, V.; Ariga, K.; *J. Mol. Catal. A: Chem.*, **2007**, *266*, 149.
17. Babitha, K. K.; Sreedevi, A.; Priyanka, K. P.; Bobby Sabu; Thomas Varghese; *IJPAP*, **2015**, *53*, 596.
18. Ranga Rao, G.; Ranjan Sahu, H.; *Proc. Indian Acad. Sci. (Chem. Sci.)*, **2001**, *113*, 651.
19. Saranya, Ramachandran; Sivasamy, A.; Dinesh Kumar, B.; *Ecotoxicol Environ Saf.*, **2016**, *134*, 445.